Electrostatic Adhesive Brakes for High Spatial Resolution Refreshable 2.5D Tactile Shape Displays

Kai Zhang and Sean Follmer

***Abstract*— We investigate the mechanism, design, modeling and fabrication of a scalable high resolution, low cost and lightweight refreshable 2.5D tactile pin array controlled by electrostatic adhesive brakes. By replacing linear actuators in motorized shape displays with a high voltage solid-state circuit that can be fabricated with printable electronics techniques, we can decrease the cost and complexity of such devices. Electrostatic adhesive brakes, made by patterning interdigital electrodes on high dielectric constant thin films, are used to hold metal pins' positions and provide contact force to the user's fingertip. We present designs of two high resolution brake modules which are 1.7 mm pitch with 0.8 mm width pins and 4 mm pitch with 1.58 mm width pins with a maximum measured dynamic loading force of 76.3 gf and static loading force of 28 gf on an individual pin (for the later size). A small demonstration of 4×2 pin array with a 4 mm pitch size within a row and 2.5 mm pitch size between the rows, using 1.58 mm width pins, was created. We also characterized the refresh time to be 37.5 ms for each brake, which enables refreshable actuated pin displays.**

I. INTRODUCTION

A. Motivation

Haptic shape perception is an important part of our everyday experience, yet it remains challenging to enable in the context of interactive haptic displays. Rich haptic shape rendering can enable immersive applications in virtual reality as well as accessible information display for people with visual impairments. Among various types of haptic devices previously investigated, encounter type haptic devices exhibit many advantages in providing haptic feedback since they are free of constraints to the user's motion and do not require the user to wear or hold any bulky devices; they instead position an end-effector or surface that a user encounters with her hand [1], [2]. Tactile shape displays are a specific class of encounter type haptic device which enable 2.5D shape rendering by controlling the heights of an 2D array of pins, creating a surface a user can explore with their hands. Applications of tactile displays include teleoperation, telepresence, 3D surface generation, games and braille systems [3], [4], [5], [6], [7].

However, the state of the art in shape display devices do not meet the design requirements for rich haptic interaction which include high resolution, large contact force, being lightweight, and low cost in addition to a large movement range of the tactile pixels (taxels) in a single device. Towards significantly improving the performance of shape displays, the following is a summary of our design goals:

The authors are with Department of Mechanical Engineering, Stanford University, 440 Escondido Mall, Stanford, CA 94305, USA E-mails: kzhang3@stanford.edu, sfollmer@stanford.edu

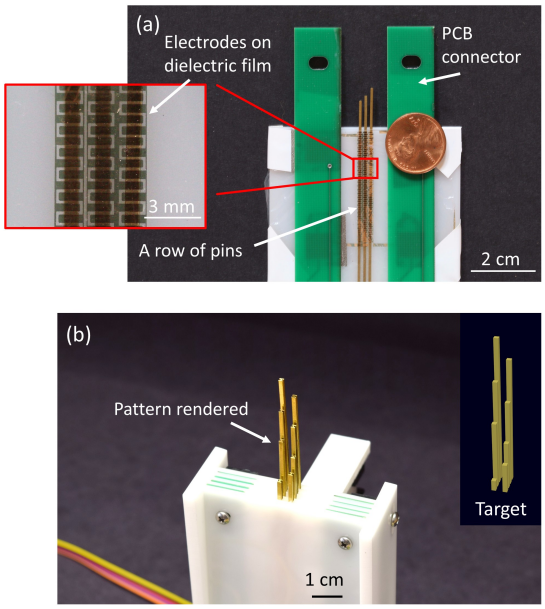

Fig. 1. (A) A row of pins with a pitch size of 1.7 mm. Two thin PCBs are used as connectors between interdigital electrodes and main control PCB. The inset figure shows a closer view of the patterned electrostatic adhesive brake. (B) Shape pattern rendered by shape display prototype. 4 rows of metal pins are packed together for a 4×2 shape display demonstrator prototype. Each pin is individually controlled by an electrostatic adhesive brake.

- Resolution: 2 - 3 mm spatial resolution to meet the requirements of fingertip perception of gross shape [8].
- Cost: extremely low cost (less than 0.10 USD) per pin so a shape display of thousands of pins can be manufactured with a price comparable to consumer electronics.
- Displacement: large dynamic movement range in the height direction to render complex 2.5D shapes.
- Force: sufficient contact force to provide robust contact while pins are perceived by the user's fingers and hands.
- Noise: low noise which will not disturb or distract users.
- Refreshable: refresh rates under 1 second to allow for interactive applications.
- Lightweight: reasonable weight so the setup can be taken with the user as a mobile device.

Most approaches to designing shape displays have relied on an individual actuator per pin and utilized electromechanical [9], [5], [6], [10], shape memory alloy [11], [12], piezoelectric [13] or hydraulic [14] actuation technologies.

However, shape displays based on brakes have unique advantages that could enable us to achieve our design goals stated above by replacing complex linear actuators with compact and low-cost brakes. While a small number of shape display systems have employed mechanical [15] or phase change [16] based brakes, these systems have been hard to manufacture or have long refresh rates. A compact solid-state circuit based solution would simplify fabrication and assembly, allow for miniaturization, and lower costs.

Thus, in this paper we investigate the use of electrostatic adhesive brakes for tactile shape displays. Leveraging the attractive force provided by electrostatic adhesion, we developed a miniaturized brake of 1.7 mm pitch size with a 0.79 mm pin width (Fig. 1(a)) and achieved maximum shear contact force of an individual pin to be 76.3 gf. Using this brake mechanism, we demonstrate a 4×2 shape display with 4 mm pitch size and 1.58 mm pin width (Fig. 1(b)). Only a single actuator is required to move all of the pins. Individual units of the shape display are controlled by deposited electrodes on a 8 µm thin dielectric film with $6.5mm \times 7mm$ transistors serving as electrical switches providing 322V voltage for each unit. To further decrease control circuit size in the future, these transistors can be as small as hundreds of micrometers in dimension. Our individual pins have a large travel distance of 3.5 cm, which provides a significant margin for shape rendering. Our electrostatic adhesive brake design is also scalable, allowing future manufacturing of large displays by utilizing printed electronic techniques, which we believe will enable our ultimate goal of a creating a low cost (less than 1000 USD), high resolution (1mm pitch), 100×100 pin array.

B. Contribution

- Demonstration of an electrostatic adhesion brake design for shape displays with a high resolution (1.7mm pitch).
- Demonstration of an integrated shape display unit with the following advantages:
  - high spatial resolution: 4 mm pitch within a row and 2.5 mm pitch between rows
  - low cost: \$0.11 USD per pin using transistor-based solid-state brake (0.09 USD for 57.8 mm^2 of PVDF based dielectric film, 0.02USD for ON MMBTA42LT1G transistor at qt. of 10,000)
  - large displacement range: 3.5 cm displacement range in the height direction
  - lightweight: using solid-state electrode brakes patterned on thin film substantially lowers weight compared to many actuation techniques
  - low noise: control of pins by the solid state circuit creates virtually no noise
- Modeling of the electrostatic adhesion brake mechanism
- Technical evaluation of contact force, refresh rate, and robustness of the electrostatic adhesion brake design and system. Maximum contact force was measured to be as high as 76.3 gf per pin for quasi-static loading and 28 gf per pin for static loading. The system takes 1.5 s to set and erase the shape pattern

C. Related Work

While much research in haptics has explored tactile displays [17], [18], [19], [20], there is substantially less research in the domain of 2.5D tactile shape displays. 2.5D tactile shape displays are encounter type haptic devices that render surface shape, size, and position by vertical displacement of an array of taxels. The discrete taxels of the shape display can be mechanically interpolated by placing an elastic material on them that smooths out the surface [5]. Some of the most important parameters in designing a shape display are number of pins, spacing, refresh rate and movement distance. Among the psychophysical and perceptual research done to figure out the design space of shape displays, two-point discrimination experiments have shown that the discrimination limit varies widely for skin on different parts of the body, while fingertips have the highest spatial sensitivity of less than 1 mm [21], [22]. Less work has studied perception of gross shape, though Shimojo et al. found ideal pin display resolution for shape perception to be 2-3mm [8].

Different actuation mechanisms have been explored to create shape displays including mechanical linear actuators [9], [5], [6], [10], electromagnets [23], shape-memory alloy (SMA) [11], [12], hydraulic [14], microelectromechanical system (MEMS) [24] and piezoelectric [25], [13]. Zhu et al. described polymer membrane actuators used as a haptic display with a spatial resolution of 1.5 mm, but the buckling amplitude of the actuator is very small at about 120 um, which constraints shape rendering ability of this actuator [26]. There are trade-offs between these different actuation techniques. Electromechanical systems using dc motors are hard to miniaturize beyond 3-5mm pitch, and they often require a conversion from rotational motion into linear motion. SMAs have high power consumption and often slow refresh rates in one direction. Thermal management is an issue for many of these technologies when they are packed closely together. Currently, there are no low-cost and high spatial resolution shape displays with active actuation.

One approach to scale the spatial resolution and cost of tactile shape displays is to replace the actuators with brakes. Brakes often offer much higher resistive force density than conventional actuators, at the expense of active force output. Xenotran created a large shape display with thousands of pins using mechanical brakes [15]. However, this system was large, costly to fabricate, and took a long time to refresh. Peters et al. demonstrated a brake-based shape display using a fusible alloy clutch which consisted of low-cost, low-melt solder heated by resistive heating elements on a printed circuit board. However, since a thermal process is required for turning the pin on and off, its refresh rate is limited[16]. To address these limitations and achieve our design goals, we explored a solid-state circuit based solution and developed an electrostatic adhesive brake for use in tactile shape displays.

II. Methods

A. Electrostatic Adhesive Brake Mechanism

Electroadhesion is an electrostatic force between two surfaces isolated by a dielectric material and was first dis-

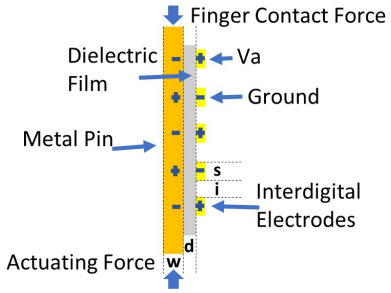

Fig. 2. Cross section of an individual electrostatic adhesive brake. Attractive force is generated by the capacitor structure which is formed by dielectric film sandwiched by metal pin and interdigital electrodes.

covered by Alfred Johnsen and Knud Rahbek in 1923 [27]. Electrostatic force is generated between a substrate material and electroadhesive pads which are conductive electrodes deposited on dielectric material. The electrodes induce an opposite charge on the substrate material, causing an electrostatic force to be generated between the two materials. In the past electroadhesion has been used in industrial applications of paper and wafer handling as well as robotic manipulation and locomotion. As a lightweight and low-energy method to provide adhesion between two surfaces, which can be dielectric or metallic, electrostatic adhesion presents an ideal choice for electrical control of an adhesive brake.

In our shape display design, we use electrostatic adhesion to create a brake mechanism that allows us to electrically control the position of individual pins with a very high spatial resolution and rapid switching speed. This electrostatic adhesive brake can be considered as a capacitor comprised of a high dielectric thin film sandwiched by a set of interdigital electrodes and a metal pin, as Fig. 2 depicts.

Since the thickness of the dielectric film is much smaller than the area of the interdigital electrodes, the electric field E in the dielectric layer can be approximated as

$$E = \frac{V_a}{2d} \tag{1}$$

where V_a is the potential difference between positive and negative electrodes of the interdigital electrodes and d is the thickness of the thin film [28]. We can calculate the charge density induced on the electrodes by Gausss law

$$\sigma = \varepsilon_r \varepsilon_0 E = \varepsilon_r \varepsilon_0 \frac{V_a}{2d} \tag{2}$$

where ε_r is the relative dielectric constant of the thin film and ε_0 is the permittivity of the vacuum.

Thus, we can calculate the electrostatic attractive force on per unit area of the pin by the following equation

$$F = -\frac{1}{2}\frac{\sigma^2}{\varepsilon_r \varepsilon_0} \tag{3}$$

Furthermore, taking into consideration the spacing between the electrodes, we denote η as the percentage of effective area required to produce an electrostatic attractive force for the total area A. The resulting electrostatic attractive force can be expressed as,

$$F = -\frac{1}{2}\varepsilon_r \varepsilon_0 A \eta (\frac{V_a}{2d})^2 \tag{4}$$

To calculate shear force supporting the pin we use the following equation,

$$F_{shear} = \mu F \tag{5}$$

where F_{shear} is the shear force and μ is the friction constant of the dielectric film. We should notice that (5) is a simplified equation since we ignore the influence of restriction force by the charges, van der Waals force and suction force between the pin and the dielectric film. A more detailed description of forces in the system can be seen in [29]. Since the measured shear force is on the same order but smaller than normal attractive force [30], we will use (5) as an engineering approximation for our model.

The maximum contact force provided to user's fingertip per unit area of shape display is another important parameter we calculate. The contact force between the end of the pin and a users finger tip should be equal to the shear force between the pin and the brake. Considering a row of pins where ratio of pin width over pitch size is β and the total length of the row is l. Then the total shear force provided by the row is

$$F = -\frac{1}{2}\mu \varepsilon_r \varepsilon_0 l \beta h_{contact} \eta (\frac{V_a}{2d})^2 \tag{6}$$

We can see shear contact force provided per unit length of the row is constant if the ratio β does not change. If we keep the distance from row to row as a constant, then the total shear force provided per unit area of the shape display will be constant if we minimize the system by decreasing the width of the pin and the pitch size by the same ratio.

To theoretically evaluate the refresh rate of our system, we consider our individual brake as a RC circuit with a resistor which connects the interdigital electrodes with the power supply and a capacitor which comes from dielectric film sandwiched by metal pin and the interdigital electrodes. Capacitance can be described by the following equation

$$C = \varepsilon_r \varepsilon_0 \frac{A\eta}{d} = \varepsilon_r \varepsilon_0 \frac{w h_{contact} \eta}{4d} \tag{7}$$

where $h_{contact}$ is height of metal pin that is in contact with the dielectric film and cross section of the metal pin is $w \times w$ (Fig. 3(a)).

We can observe that capacitance of an individual brake will decrease as we decrease the width w of the metal pin. If we keep the connecting resistance as a constant value then we will have a smaller RC constant and a faster refresh rate if we minimize the size of each individual pin and brake.

B. Design of an Individual Electrostatic Adhesive Brake

After describing the system with the abstract model above, we will now discuss our design in the context of the constraints of real components and fabrication techniques.

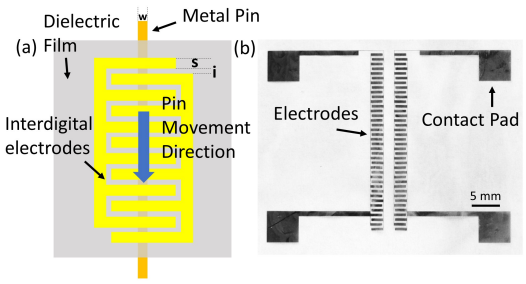

Fig. 3. (A) Schematic showing movement direction of metal pin relative to interdigital electrodes. Electrodes are designed vertically to the pin's movement to provide the largest shear force. (B) 50 nm of gold interdigital electrodes sputtered on 8 µm PVDF-TrFE-CFE terpolymer dielectric film.

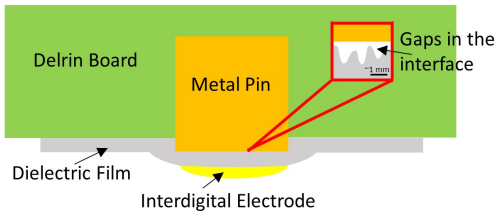

Fig. 4. Top view of electrostatic adhesive brake. Dielectric film is fixed to Delrin board at the left and right side while middle part of the film has flexibility to deform so small gaps between dielectric film and metal pin can be removed

Since our electrostatic adhesive brake serves as a switch to hold the pin at a specific position and provide contact force to user's fingertip (through shear force between the pin and the brake), we designed the interdigital electrodes perpendicular to the direction of the pins movement direction which has been demonstrated to generate the largest attractive force when the pin starts to fall off of the adhesive [30] (Fig. 3(a)). To optimize the effective contact area for generating electrostatic adhesion force, we designed our interdigital electrodes as Fig. 3(b) shows. The electrodes are patterned as dense as possible to minimize empty areas which do not provide attractive forces in the switching process. The width of our interdigital electrodes, s in Fig. 3(a), is designed to be 500 µm, based on experimental results from [28]. To determine the interval between parallel electrodes, we empirically tested the break down voltage between parallel electrodes on the dielectric film at different voltages and determined 120 µm to be the minimum gap within safety limits when operating at 322V. Thus the interval between parallel electrodes, i in Fig. 3(a), was designed to be 300 µm and corners of the electrodes were rounded to avoid sparks.

As we can observe from (4), adhesion force is proportional to the square power of the applied voltage and inversely proportional to the square of the thickness of the dielectric layer. Thus we use a very thin dielectric film of 8 µm thickness with a relatively large dielectric constant of 50 (PolyK Technologies P(VDF-TrFE-CFE)) to maximize electrostatic adhesive force in our individual brake. We did not use dielectric films thinner than 8 µm in our prototypes and testing because the mechanical strength of those films are not ideal and are easier to break during the assembly process.

Though we can further increase the voltage in our system for a larger contact force, we decide to set our voltage to 322 V due to low cost, safety, minimization of sparking, and transistor miniaturization considerations.

In our setup, pins have a width of 1.58 mm while interdigital electrodes have a height of 34.0 mm. We choose the width of the pins to be as small as possible to increase the resolution of our shape display, while still accounting for constraints on pin axis straightness and stiffness. Maximum contact force provided by the interdigital electrodes is directly proportional to contact area between interdigital electrodes and metal pins. Thus, to increase contact area a larger height of interdigital electrodes is desirable. However, due to limitations on total device size, and decreased performance with high aspect ratio pins, we fixed the height of the interdigital electrodes to be 34.0 mm. Accounting for the spacing between interdigital electrodes to prevent sparks, the total contact surface area between pin and interdigital electrodes is 33.6 mm^2. Thus, the theoretical shear contact force provided between the pin and the dielectric film based on (5) is 60.2 gf considering a voltage of 322 V and the dielectric film's friction constant μ of about 0.2 [1]. Compared with the small weight of our pin (about 1 gf), this gives us a very large margin to choose a voltage and other design parameters in our system to support a user's interaction force.

In our system, it is essential to provide good contact between the pins and the dielectric film since any air gap between them will significantly reduce the attractive force. Fig. 4 depicts the top view of an individual electrostatic adhesive brake, a dielectric film with interdigital electrodes is fixed to a Delrin frame at the left and right side while middle part of the film has the flexibility to deform and fit to the metal pin locally. This design helps remove small gaps between dielectric film and the metal pin, since attractive forces between them will hold them together tightly, which will further increase attractive force. If we directly apply the dielectric film to a rigid substrate, our experiments show that small curvature and surface roughness differences between the metal pin and the substrate will significantly decrease the force between them. Our device structure in Fig. 4 also constrains the metal pin inside the groove so that it can support tangential forces.

C. System Design Principles

In the following section, we discuss integrating individual electrostatic adhesive brakes into a shape display system. Fig. 5 shows cross section of our system. Multiple pins will initially be placed on a platform driven by a linear actuator. During the process of shape rendering, the linear actuator will drive all the pins to the highest position. As the linear actuator starts to lower the pins, some of the pins will be adhered to the activated electrostatic adhesive brakes behind,

[1] https://www.plasticsintl.com/datasheets/KYNAR%20740%20PVDF.pdf

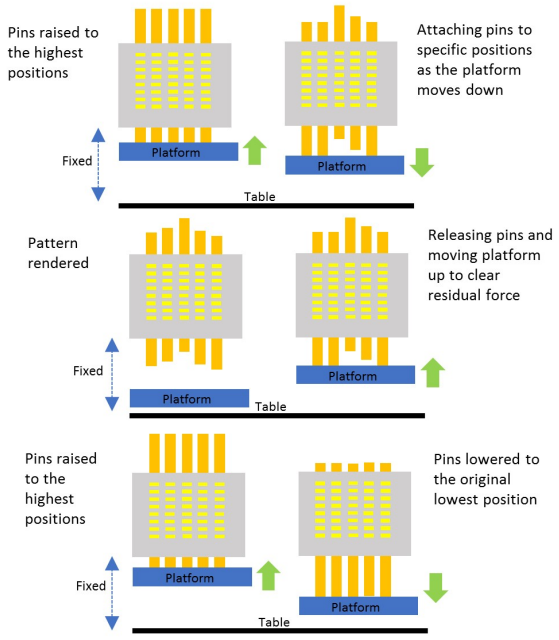

Fig. 5. Shape rendering process flow of our shape display prototype.

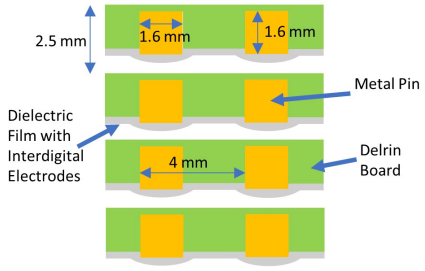

Fig. 6. Top view of the shape display demonstration system.

them while others will still stay on the platform. Before the platform arrives to the lowest position, all the pins will be attached to the dielectric film and render the desired shape. To reset the pins, firstly we reverse direction of the high voltage back and forth for many cycles to remove most of the residual charges on the pin. Then we raise the platform up to the highest position to further remove all the residual force and enforce the pins to leave the dielectric film. At the last step, we lower the platform down to its original position at the lowest place.

We constrain the movement of the rectangular pins to be in the vertical direction with vertical grooves, creating a prismatic joint, as the top view of our system in Fig. 6 shows.

These grooves prevent pins from touching each other with a thin wall separating them. Rows of pins are packed together as Fig. 6 shows. The grooves are designed to be a little shallower than the thickness of the pin so that part of the pin will extend outside of the groove, which helps to improve contact between the dielectric film and metal pins.

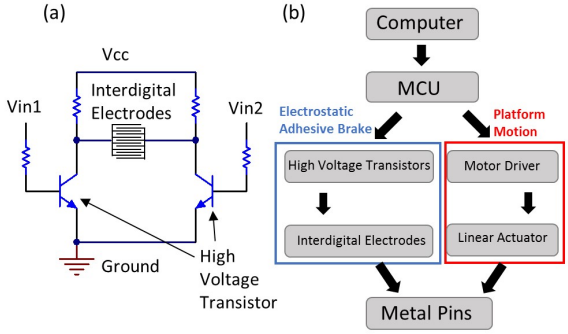

Fig. 7. (A) Circuit diagram of an individual electrostatic adhesive brake. (B) System diagram of our electrical and mechanical control system.

In our setup, every pin is controlled by two transistors as Fig. 7(a) depicts. This design helps to reduce the residual charges on the pins when the DC high voltage is turned off [30]. In the process of attaching the pin to the dielectric film, we apply a high voltage to the pin by setting one transistor on and the other transistor off. When releasing the pin, we apply a reverse high voltage across the interdigital electrode to help neutralize the residual charges and then switch the direction of the high voltage again to further release the charges. By switching high voltage direction back and forth for 1000 cycles in a second, we have obtained a very low residual force [30]. To avoid residual forces caused by the DC high voltage, another choice is directly use AC high voltage across the interdigital electrodes to adhere metal pins. But this method will reduce the attractive force between the pin and the dielectric film. Thus, we drive the system with a combination of DC and AC voltage as described above.

Fig. 7(b) shows block diagram of our shape display system. High voltage transistors and a motor driver are controlled by a microcontroller connected to a computer. We set the position of the pins by computationally controlling the linear actuator and the interdigital electrode brakes synchronously.

D. Manufacturing and Assembly

We built our shape display system by firstly assembling a row of pins as Fig. 1(a) shows. In our shape display prototype, two grooves of 1.21 mm deep and 1.9 mm wide were milled on a 1.98 mm thick Delrin board by our Othermill CNC tool. The grooves are designed to be a little bit shallower than the thickness of the pin as we discussed in the system design principles section. The grooves are also slightly wider than the pins so that metal pins can move up and down smoothly in the grooves without a large friction. Brass H-Column pins are cut to be 14 cm long so that they can afford a good movement distance of 3.5 cm in height direction. In theory, the pins can be even longer than 14 cm but at the same time they need to be very straight so they can fit in the mechanical tolerance of the grooves constraining them.

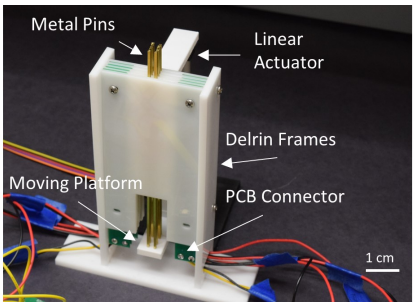

Fig. 8. Assembled shape display system. One linear actuator is used to move the platform underneath the metal pins. Interdigital electrodes are connected by conducting wires from the bottom of the setup which are furthered connected with main control PCB.

To fabricate the interdigital electrodes with a 500 µm width and 300 µm gap, P(VDF-TrFE-CFE) film of 8 µm thickness was deposited with a 50 nm layer of gold. Laser ablation was used to remove part of the gold layer on the surface of the dielectric film, thus forming the interdigital electrodes and contact pads as we designed. Then we applied the dielectric film, with the patterned electrodes, to the Delrin frame and tuned the tightness of the stretched dielectric film carefully to be approximately 1% strain, so that it is not too loose to provide good contact with the metal pins and not too tight to generate a large frictional force durring the movement of the metal pins.

To route the interdigital electrodes to our control PCB board, we use another two 500 µm thin PCB boards as the connectors for a row of pins. These two boards also provide mechanical support between Delrin boards so that the metal pins from the front Derlin board will not touch the Delrin board behind it. Double sided conductive tape is used as conductive adhesive layer between the thin PCB board and the contact pads (electrically routed to the interdigitated electrodes) on our dielectric film.

After assembling a row of pins, we packed 4 Delrin frames together to form a 4×2 electroadhesive shape display as shown in Fig. 8. Stranded wires were soldered to the pads on the thin PCB board and routed through the bottom part of the setup to the control PCB board.

Our main PCB board consists of one microcontroller (PJRC Teensy 3.6), 9 transistors (STMicroelectronics STN0214) and 18 resistors to control the 8 pin system. Though in theory every pin needs to be controlled by two transistors, we share ground of the interdigital electrodes, thus 9 transistors will be sufficient for our voltage switching process. Due to safety and low power consumption considerations, 5 MΩ resistors are connected between interdigital electrode and power supply so that the current charging the pad of each interdigital electrode will be 64.4 µA, which means our 4×2 pins array only consumes 0.166 W of power at 322V voltage.

To provide a voltage of 322V for electrostatic adhesion, an high voltage DC converter (EMCO AG05p-5) is connected between power supply and the PCB board. High voltage transistors with a maximum collector-emitter voltage of 1400V ($V_{BE} = 0$) are applied in our circuit so that we can achieve an on/off control of the high voltage across each brake by turning the transistors on/off with the microcontroller which is further programmed and controlled by an Arduino program on the computer.

A linear actuator (Actuonix L12) is connected to a motor driver board (TI DRV8833), which is further controlled by the microcontroller on our main PCB board, enabling movement of the linear actuator and the attaching/releasing state of each pin to be synchronized.

III. Results Analysis

A. Pattern Rendering Results

Fig. 9 shows multiple shape patterns we rendered with our shape display prototype with the target shape on the top right corner of each figure. From the results we can observe that with our shape display, shapes with fine and sharp features can be achieved due to the high resolution and large linear displacement of our device.

B. Quasi-static Loading

The maximum contact force provided on the tip of the metal pin before the adhesion fails and the pin slides is an important parameter for our shape display. In a real interaction application scenario, a large contact force will significantly improve haptic exploration with the shape display. Thus, we measured the value of the maximum contact force on metal pin's tip by quasi-statically loading it. A horizontal groove on a Delrin board was used to constrain movement of the metal pin while a linear actuator mounted with a force sensor (Honeywell FSG005WNPB 9.8 mN sensitivity) pushed the pin forward and measured the contact force at the same time. To measure the maximum contact force, a metal pin was attached to dielectric film by activating the electrostatic brake. Once the linear actuator hit the metal pin, we monitored the reading from the force sensor. The velocity of our linear actuator was very slow (1.9 mm/s) so the measurement process can be considered as a quasi-static process. Since the linear actuator provided a force significantly larger than our brake, the metal pin was eventually removed from the brake by linear actuator. The maximum force measured before the

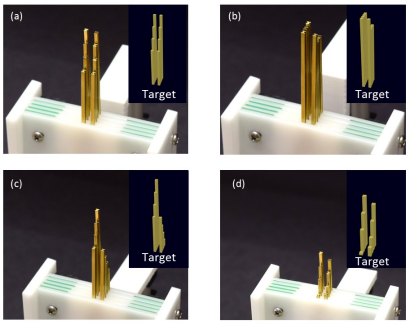

Fig. 9. Rendering of four different shape patterns. Target shape is shown on the top right corner of each figure.

TABLE I
QUASI-STATIC LOADING FORCE MEASUREMENT RESULTS

Electrode Density	Metal Pin Width	Measured	Model
High	1.58 mm	76.3 gf	59.6 gf
Low	1.58 mm	65.0 gf	53.1 gf
High	0.79 mm	39,1 gf	39.3 gf

brake was removed is defined as maxiumum contact force. Table I sumerizes our measurement results and the modeled results from (5). Our high density electrodes have a width of 480 µm and a gap of 120 µm while our low density electrodes have more empty area with a width of 500 µm and gap of 300 µm.

Considering an individual brake has a friction force of 0.67 gf in our setup when voltage is turned off due to friction between metal pin, dielectric film and Delrin board, the on/off ratio of force our brake resists is very large. Our measured force is larger than theoretical calculated result becuase we used a simplified engineering model ignoring restricting force, Van der Waals force and suction force which are difficult to evaluate in this situation [29].

In real applications the user's fingertip is supposed to be in contact with multiple pins while haptically exploring the shape. Considering our shape display has a pitch size of 4 mm within a row and 2.5 mm between rows and assuming a user's finger tip has an area of 16 mm $\times$ 12 mm, there will be approximately 20 pins in touch with user's fingertip which means the maximum contact force can be as high as 76.3 gf $\times$ 20 = 1526 gf. This force is large enough for user to explore small features on a surface where the usual contact force for this purpose is 51 gf [31].

C. Refresh Rate Analysis

As discussed in the system design principle section, we set the positions of the pins by turning on the voltage when the pins stop at a specific position which we call a level. Thus, the total time for us to set the positions of the pins is dependent on how many different levels pins will be configured to for a given shape, how long it takes to activate the brake, and also the speed of our linear actuator.

To measure the delay time between the time we send a signal to the pin and when the pin is attached to the film, we used a high speed camera (1200 frames per second) to monitor the whole process. An LED was wired to turn on once high voltage was applied across the pin. The delay time for pin attachment was measured as the interval starting when the LED was turned on to when the the pin was observed to start leaving the platform. Using this method, the observed delay time was 37.5 ms when using 355V and actuating the platform at a speed of 25 mm/s. In reality, the delay time could be even smaller than this because the high speed camera has a relatively low resolution of 1 mm at this distance. We take 37.5 ms as the upper bound of our delay time since we let the pin move for a significant distance in the picture so that we can clearly tell it departed from the linear actuator. Since we have a maximum of 8 levels to set in our demonstrator system, the total delay time by attaching the pins is less than 37.5 ms $\times$ 8 = 300ms. Considering our linear actuator moves with a maximum speed of 25 mm/s and our dynamic range in the height direction is 3.5 cm, it takes our linear actuator 1.4 s to travel the distance. Thus the delay time of setting our pins is still relatively small in terms of the total time required to refresh the display.

From (7), the capacitance of an individual brake in our system is calculated as 2.5 nF. Since we use a resistor of 5 MΩ to connect each interdigital electrode to the power supply, the RC constant of our system is 12.5 ms. This calculated value is in the same order of magnitude as what we observed.

The measured sliding distance of the metal pin after we attached it to the dielectric film was observed to be less than 90 µm. This ensures that we have accurate control of our pin positions in the shape rendering process.

D. Robustness of the System

To characterize robustness of our device, we carried out a test where we repeated the shape rendering process flow of an individual electrostatic adhesive brake and pin, shown in Fig. 5. The test was carried out on two separate days with a total of 1602 cycles of the shape rendering process until the first failure was observed. This failure was due to the interdigital electrode not holding up the metal pin despite a high voltage still being applied. However, when we turned off the voltage and restarted the process after 1 minute, our setup still worked well as we expected. The shear contact force our brake provided was measured as 65 gf after we carried out 1700 cycles of the robustness test. This demonstrates our setup has a good robustness in shape rendering and providing contact forces to the user.

When perceiving shapes rendered from our shape display prototype, users will tap or apply a force to the metal pins many times by their hand with a certain amount of contact force. Thus we carried out a repeatability test to characterize robustness of our device when we load and unload a weight on an individual electrostatic adhesive brake for many cycles as Table II shows. Three interdigital electrodes fabricated in the same batch were repeatably loaded and unloaded with 13 gf, 18 gf and 23 gf of weight, respectively. As we can observe from the results, our individual brakes displayed very good repeatability in the 13 gf and 18 gf weight conditions. We did not observe any sliding of the metal pin during our test of 1021 cycles. When we increased our weight to 23 gf force, the metal pin slid down after 80 cycles of loading and unloading the weight. Considering resolution of our shape display, user's fingertips will be in contact with about 20 metal pins during the shape perception process, the static loading test demonstrates our device has a good ability in providing a shape pattern with large contact force in a repeatable way.

During shape display, the metal pin should not move relative to the dielectric film once the high voltage is turned on. If the user applies a large force to the pin and the brake

TABLE II
STATIC LOADING FORCE MEASUREMENT RESULTS

Loading Weight	Cycles Before Failure
13 gf	more than 1021 times
18 gf	more than 1021 times
23 gf	80 times

fails when the high voltage is not turned off, the contact force provided by the brakes can degrade over time. This is due to charging of the metal pin when it slides along the film with high voltage on. We observed that after 5 brake failures, shear contact force provided by the metal pin decreased to 70 % of the original value. However, after grounding the charged pin to remove the accumulated charges, the shear contact force recovered to its original value.

IV. CONCLUSION

We demonstrated the design and implementation of a novel electrostatic adhesive brake for tactile shape displays with the advantage of high resolution, low cost, large contact force, low noise and lightweight performance. We evaluated its shape rendering ability by measuring contact force, refresh rate and robustness.

In the future we will investigate scaling our shape display up to a palm size device with 100×100 pins. We believe there are no fundamental limitations to building a larger scale shape display using the proposed design. However, a better mechanical design and a more complex control circuit will be required. In addition, we will explore improvements to the refresh rate of our system by investigating path planning algorithms to optimize movement of the pins.

REFERENCES

[1] W. A. McNeely, "Robotic graphics: a new approach to force feedback for virtual reality," in *Virtual Reality Annual International Symposium, 1993., 1993 IEEE*. IEEE, 1993, pp. 336–341.

[2] H. Hoshino, R. Hirata, T. Maeda, and S. Tachi, "A construction method of virtual haptic space (ii)," *Proceedings of ICAT/VRST*, vol. 95, pp. 211–220, 1995.

[3] E. Y. Chen and B. A. Marcus, "Exos slip display research and development," in *Proceedings of the International Mechanical Engineering Congress and Exposition*, 1994, pp. 55–1.

[4] E. Petriu and W. McMath, "Tactile operator interface for semi-autonomous robotic applications," *AIRAS, Artificial Intelligence, Robotics and Automation, Space*, pp. 77–82, 1992.

[5] C. R. Wagner, S. J. Lederman, and R. D. Howe, "A tactile shape display using rc servomotors," in *Haptic Interfaces for Virtual Environment and Teleoperator Systems, 2002. HAPTICS 2002. Proceedings. 10th Symposium on*. IEEE, 2002, pp. 354–355.

[6] H. Iwata, H. Yano, F. Nakaizumi, and R. Kawamura, "Project feelex: adding haptic surface to graphics," in *Proceedings of the 28th annual conference on Computer graphics and interactive techniques*. ACM, 2001, pp. 469–476.

[7] D. Overholt, "The matrix: a novel controller for musical expression," in *Proceedings of the 2001 conference on New interfaces for musical expression*. National University of Singapore, 2001, pp. 1–4.

[8] M. Shimojo, M. Shinohara, and Y. Fukui, "Human shape recognition performance for 3d tactile display," *IEEE Transactions on Systems, Man, and Cybernetics-Part A: Systems and Humans*, vol. 29, no. 6, pp. 637–644, 1999.

[9] M. Shinohara, Y. Shimizu, and A. Mochizuki, "Three-dimensional tactile display for the blind," *IEEE Transactions on Rehabilitation Engineering*, vol. 6, no. 3, pp. 249–256, 1998.

[10] S. Follmer, D. Leithinger, A. Olwal, A. Hogge, and H. Ishii, "inform: dynamic physical affordances and constraints through shape and object actuation." in *ACM UIST 2013*, vol. 13, 2013, pp. 417–426.

[11] I. Poupyrev, T. Nashida, S. Maruyama, J. Rekimoto, and Y. Yamaji, "Lumen: interactive visual and shape display for calm computing," in *ACM SIGGRAPH 2004 Emerging technologies*. ACM, 2004, p. 17.

[12] M. Nakatani, H. Kajimoto, D. Sekiguchi, N. Kawakami, and S. Tachi, "3d form display with shape memory alloy." in *ICAT*, vol. 8, 2003, pp. 179–184.

[13] S. Jang, L. H. Kim, K. Tanner, H. Ishii, and S. Follmer, "Haptic edge display for mobile tactile interaction," in *Proceedings of the 2016 CHI Conference on Human Factors in Computing Systems*. ACM, 2016, pp. 3706–3716.

[14] H. Zhu and W. J. Book, "Practical structure design and control for digital clay," in *ASME 2004 International Mechanical Engineering Congress and Exposition*. American Society of Mechanical Engineers, 2004, pp. 1051–1058.

[15] C. Carlberg, "Clutch mechanism for a raised display apparatus," Oct. 21 2008, uS Patent 7,439,950.

[16] B. J. Peters, "Design and fabrication of a digitally reconfigurable surface," Ph.D. dissertation, MIT, 2011.

[17] F. Vidal-Verdú and M. Hafez, "Graphical tactile displays for visually-impaired people," *IEEE Transactions on neural systems and rehabilitation engineering*, vol. 15, no. 1, pp. 119–130, 2007.

[18] V. Hayward and M. Cruz-Hernandez, "Tactile display device using distributed lateral skin stretch," in *Proceedings of the haptic interfaces for virtual environment and teleoperator systems symposium*, vol. 69, no. 2. ASME, 2000, pp. 1309–1314.

[19] Q. Wang and V. Hayward, "Compact, portable, modular, high-performance, distributed tactile transducer device based on lateral skin deformation," in *Haptic Interfaces for Virtual Environment and Teleoperator Systems, 2006 Symposium on*. IEEE, 2006, pp. 67–72.

[20] M. Benali-Khoudja, M. Hafez, J.-M. Alexandre, and A. Kheddar, "Tactile interfaces: a state-of-the-art survey," in *Int. Symposium on Robotics*, vol. 31, 2004, pp. 23–26.

[21] I. M. Koo, K. Jung, J. C. Koo, J.-D. Nam, Y. K. Lee, and H. R. Choi, "Development of soft-actuator-based wearable tactile display," *IEEE Transactions on Robotics*, vol. 24, no. 3, pp. 549–558, 2008.

[22] K. O. Johnson and J. R. Phillips, "Tactile spatial resolution. i. two-point discrimination, gap detection, grating resolution, and letter recognition," *Journal of neurophysiology*, vol. 46, no. 6, pp. 1177–1192, 1981.

[23] J. J. Zárate and H. Shea, "Using pot-magnets to enable stable and scalable electromagnetic tactile displays," *IEEE transactions on haptics*, vol. 10, no. 1, pp. 106–112, 2017.

[24] T. Ninomiya, K. Osawa, Y. Okayama, Y. Matsumoto, and N. Miki, "Mems tactile display with hydraulic displacement amplification mechanism," in *Micro Electro Mechanical Systems, 2009. MEMS 2009. IEEE Conference on*. IEEE, 2009, pp. 467–470.

[25] K.-U. Kyung, M. Ahn, D.-S. Kwon, and M. A. Srinivasan, "A compact broadband tactile display and its effectiveness in the display of tactile form," in *Eurohaptics Conference, 2005 and Symposium on Haptic Interfaces for Virtual Environment and Teleoperator Systems, 2005. World Haptics 2005. First Joint*. IEEE, 2005, pp. 600–601.

[26] R. Zhu, U. Wallrabe, M. C. Wapler, P. Woias, and U. Mescheder, "Dielectric electroactive polymer membrane actuator with ring-type electrode as driving component of a tactile actuator," *Procedia Engineering*, vol. 168, pp. 1537–1540, 2016.

[27] A. Johnsen and K. Rahbek, "A physical phenomenon and its applications to telegraphy, telephony, etc." *Journal of the Institution of Electrical Engineers*, vol. 61, no. 320, pp. 713–725, 1923.

[28] K. Yatsuzuka, F. Hatakeyama, K. Asano, and S. Aonuma, "Fundamental characteristics of electrostatic wafer chuck with insulating sealant," *IEEE Transactions on Industry Applications*, vol. 36, no. 2, pp. 510–516, 2000.

[29] J. Guo, T. Bamber, M. Chamberlain, L. Justham, and M. Jackson, "Optimization and experimental verification of coplanar interdigital electroadhesives," *Journal of Physics D: Applied Physics*, vol. 49, no. 41, p. 415304, 2016.

[30] K. Asano, F. Hatakeyama, and K. Yatsuzuka, "Fundamental study of an electrostatic chuck for silicon wafer handling," *IEEE Transactions on Industry Applications*, no. 3, pp. 840–845, 2002.

[31] A. M. Smith, G. Gosselin, and B. Houde, "Deployment of fingertip forces in tactile exploration," *Experimental brain research*, vol. 147, no. 2, pp. 209–218, 2002.